Ubiquitin-dependent degradation of HDAC4, a new regulator of random cell motility

Nadia Cernotta*, Andrea Clocchiatti*, Cristina Florean*, and Claudio Brancolini
Dipartimento di Scienze e Tecnologie Biomediche, Sezione di Biologia and MATI Center of Excellence, Università degli Studi di Udine, Udine 33100, Italy

ABSTRACT **HDAC4 (histone deacetylase 4) belongs to class IIa of histone deacetylases, which groups important regulators of gene expression, controlling pleiotropic cellular functions. Here we show that, in addition to the well-defined nuclear/cytoplasmic shuttling, HDAC4 activity is modulated by the ubiquitin–proteasome system. Serum starvation elicits the poly-ubiquitination and degradation of HDAC4 in nontransformed cells. Phosphorylation of serine 298 within the PEST1 sequence plays an important role in the control of HDAC4 stability. Serine 298 lies within a glycogen synthase kinase 3β consensus sequence, and removal of growth factors fails to trigger HDAC4 degradation in cells deficient in this kinase. GSK3β can phosphorylate HDAC4 in vitro, and phosphorylation of serine 302 seems to play the role of priming phosphate. We have also found that HDAC4 modulates random cell motility possibly through the regulation of KLF2 transcription. Apoptosis, autophagy, cell proliferation, and growth arrest were unaffected by HDAC4. Our data suggest a link between regulation of HDAC4 degradation and the control of cell motility as operated by growth factors.**

Monitoring Editor
William P. Tansey
Vanderbilt University

Received: Jul 7, 2010
Revised: Nov 12, 2010
Accepted: Nov 15, 2010

INTRODUCTION

Lysine acetylation is emerging as a widespread posttranslation modification (PTM) involved in the regulation of several cellular functions (Choudhary *et al.*, 2009). Histone deacetylases (HDACs) are an assorted family of nuclear and cytoplasmic enzymes involved in reversing this PTM. The HDAC family can be clustered into distinct classes based on sequence and structural homologies to yeast enzymes Rpd3, Hda1, and Sir2 (Yang and Grégoire, 2005). HDAC4 is a member of class IIa, which is characterized by homologies with yeast Hda1, nuclear cytoplasmic shuttling, and heterogeneous levels of expression in various tissues. Similarly to other class IIa members, HDAC4 contains intrinsic nuclear import and export sequences on which converge distinct signaling pathways to modulate its repressive influence (Yang and Seto, 2008).

HDAC4 impinges on multiple and apparently contradictory cellular fates, including differentiation, apoptosis, survival, cell growth, and proliferation (Paroni *et al.*, 2004; Vega *et al.*, 2004; Bolger and Yao, 2005; Backs *et al.*, 2006; Paroni *et al.*, 2007; Wilson *et al.*, 2008; Cadot *et al.*, 2009; Chen and Cepko, 2009). Not surprisingly, multiple levels of regulation mirror this exaggerated versatility. The control of HDAC4 nuclear cytoplasmic shuttling seems to be the master option for modulating its activity (Paroni *et al.*, 2004; Ago *et al.*, 2008). As reported in several studies, HDAC4 nuclear cytoplasmic shuttling is under the control of different kinases and phosphatases, in cooperation with 14–3-3 proteins. Phosphorylation/dephosphorylation cycles efficiently and rapidly couple the repressional activity of class IIa HDACs to environmental signals (Grozinger and Schreiber, 2000; Wang *et al.*, 2000; McKinsey *et al.*, 2001; Martin *et al.*, 2008; Paroni *et al.*, 2008; Yang and Seto, 2008).

HDAC4 activities can be modulated by additional strategies. In colon, HDAC4 is massively expressed in the proliferative compartment and is down-regulated during intestinal differentiation (Wilson *et al.*, 2008). In muscle, denervation modulates HDAC4 expression (Cohen *et al.*, 2009; Tang *et al.*, 2009).

Despite changes in HDAC4 levels having been observed in different situations, the mechanisms responsible for such fluctuations are poorly defined. Sp1 and Sp3 transcription factors regulate HDAC4 transcription, but how this control integrates with cellular signaling networks is unclear (Liu *et al.*, 2006). In addition, posttranscriptional strategies to modulate HDAC4 mRNA levels also exist;

This article was published online ahead of print in MBoC in Press (http://www.molbiolcell.org/cgi/doi/10.1091/mbc.E10-07-0616) on November 30, 2010.

*These authors contributed equally to this work.

Address correspondence to: Claudio Brancolini (claudio.brancolini@uniud.it).

Abbreviations used: Gas2, growth arrest specific gene 2; GSK3β, glycogen synthase kinase 3β; HDAC, histone deacetylase; KLF2, Krüppel-like factor 2; LC3, light chain 3; MEF2, myocyte-enhancer factor 2; PCNA, proliferating cell nuclear antigen; PTM, posttranslation modification; QRT-PCR, quantitative real-time PCR.

for example, miR-1 contributes to repress HDAC4 levels during muscle differentiation (Sun *et al.*, 2010).

Here we have investigated the expression levels of HDAC4 in response to growth factors. We have discovered that growth factor deprivation elicits poly-ubiquitination and proteasome-mediated degradation of HDAC4. Serines at position 298 and 302 and the kinase glycogen synthase kinase 3β (GSK3β) seem to be important elements of the signaling pathway governing HDAC4 stability. Finally, we have explored which among the different cellular responses under serum regulation, such as autophagy, apoptosis, cell cycle, and motility could be influenced by HDAC4. Our results suggest that HDAC4 regulates random cell motility. Overall this study discovers a new mechanism of HDAC4 regulation and provides a link between HDAC4 degradation and the decline of cell motility elicited by growth factor withdrawal.

RESULTS

Growth factors modulate HDAC4 expression levels in normal breast cells

In the immortalized, nontransformed mammary epithelial cell line MCF-10A, proliferation is modulated by exogenously added growth factors. We used MCF-10A cells to evaluate the effect of growth factors on the expression levels of HDAC4. Cells were grown for 24 h in complete medium; next serum and additional growth factors were removed. Growing MCF-10A cells for another 48 h in low serum (0.5% fetal bovine serum [FBS]) promotes exit from the cell cycle, as evidenced by proliferating cell nuclear antigen (PCNA) down-regulation (Figure 1A). HDAC4 levels were similarly down-regulated. Next we evaluated the effect of different medium components on HDAC4 levels. Addition of hydrocortisone, insulin, and cholera toxin was sufficient to sustain HDAC4 and PCNA expression in low serum. Curiously some increase in HDAC4 but not in PCNA levels can be seen after supplementing low serum medium with cholera toxin and hydrocortisone (Figure 1A). Re-addition of growth factors to MCF-10A–starved cells promoted cell proliferation and HDAC4 expression (unpublished data).

To evaluate changes in the amount of HDAC4 transcripts by low serum, we used quantitative real-time PCR (QRT-PCR) analysis. RNA was extracted from growing MCF-10A cells (cultured for 24 h in complete medium) or from cells cultured for different times in 0.5% FBS. As shown in Figure 1B, HDAC4 mRNA levels were unaffected by growth factor removal.

Having excluded changes in mRNA levels, HDAC4 down-regulation after serum starvation could be the consequence of proteolysis or of translation control. To discriminate between these possibilities, MCF-10A cells were cultured in low serum in the presence of the proteasome inhibitor MG132. Figure 1B confirms that serum starvation and elimination of growth factors elicit the down-regulation of HDAC4, already evident 24 h after the removal. Growing cells for an additional 24 h in low serum further decreased HDAC4 levels. This down-regulation was efficiently prevented by the presence of MG132.

To understand whether HDAC4 is also degraded via the ubiquitin–proteasome system in the presence of growth factors, MCF-10A cells were grown for 48 or 72 h in complete medium in the presence or not of MG132. Figure 1D shows that, in this case, HDAC4 levels were not increased after proteasomal inhibition.

Cancer cells also can proliferate in the presence of limited amounts of growth factors. Interestingly, HDAC4 levels were unaffected in the breast cancer cell line MCF-7, cultured in low serum conditions (Figure 1E). Similar results were obtained with the glioblastoma cell line U87MG. Hence degradation of HDAC4, as elicited by the absence of growth factors, is a prerogative of nontransformed cells.

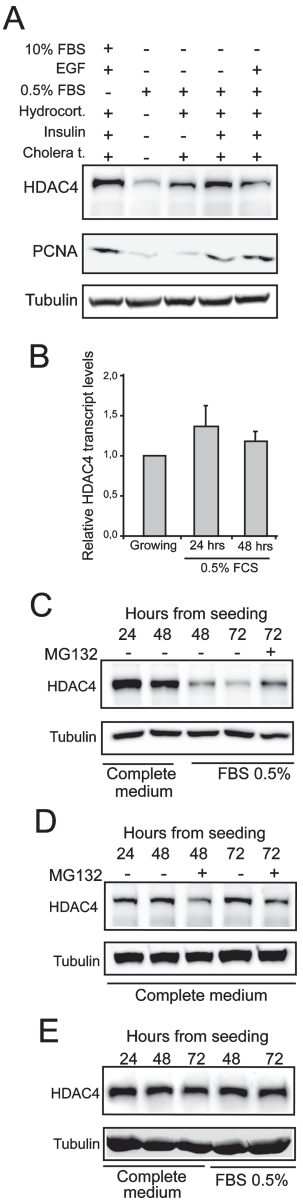

FIGURE 1: Proteasomal-dependent degradation of HDAC4 upon growth factor removal. (A) MCF-10A cells were grown in complete medium for 24 h (lane 1). Next cells were incubated with different media, as indicated, for another 48 h. Cellular lysates were generated and subjected to immunoblot analysis using the specific antibodies. Tubulin was used as loading control. (B) Regulation of HDAC4 mRNA expression by low serum. MCF-10A cells were grown in complete medium for 24 h or in low serum for an additional 24 and 48 h. RNA was extracted, and QRT-PCR analysis was performed to quantify HDAC4 mRNAs. Samples were normalized to GAPDH (means ± SD, n = 4). (C) MCF-10A cells were grown in complete medium for 24 h or in low serum for an additional 24 or 48 h. MG132 (2.5 μM) was added to cells 24 h before cell lysis. Cellular lysates were subjected to immunoblot analysis using anti-HDAC4 antibodies. Tubulin was used as loading control. (D) MCF-10A cells were grown in complete medium for the indicated times. When used, MG132 (2.5 μM) was added to cells 24 h before cell lysis. Cellular lysates were generated and subjected to immunoblot analysis using anti-HDAC4 antibodies. Tubulin was used as loading control. (E) MCF-7 breast cancer cells 24 h after seeding were maintained in 10% FBS (complete medium) or grown in low serum (0.5% FBS) for the indicated times. Cellular lysates were generated and subjected to immunoblot analysis using anti-HDAC4 antibodies. Tubulin was used as loading control.

Proteasome-dependent degradation of HDAC4 in NIH3T3 cells during growth arrest induced by serum starvation

To confirm that proteasome-dependent degradation of HDAC4 in response to serum deprivation is not limited to MCF-10A cells, we used NIH3T3 murine fibroblasts. Initially we evaluated HDAC4 levels in cells grown for 24 h in 10% FBS (growing cells) and following 24 or 48 h of culture in low serum conditions. MG132 was used to evaluate the contribution of the ubiquitin-dependent degradation. Figure 2A demonstrates that serum starvation also promotes proteasomal degradation of HDAC4 in NIH3T3 cells. Similarly to what was observed in MCF-10A cells, HDAC4 was selectively targeted to the proteasome only when serum was removed. In fact, addition of MG132 to actively proliferating cells does not influence HDAC4 levels (Figure 2B).

We also analyzed whether serum starvation modulates the subcellular localization of HDAC4 and whether interfering with HDAC4 degradation could influence its nuclear accumulation. In growing cells, HDAC4 shows a cytoplasmic localization in the majority of the cells. A pancellular localization can be observed in a limited number of cells, whereas rare cells accumulate HDAC4 in the nucleus (Figure 2C). In serum-starved cells, HDAC4 levels were clearly reduced. When we performed a quantitative analysis (unpublished data), however, the subcellular localization was unchanged compared to growing cells. Treatment of serum-starved cells with leptomycin B, an inhibitor of CRM1-mediated nuclear export, elicited the nuclear accumulation of HDAC4 (Figure 2C) similarly to growing cells (unpublished data). This result demonstrates that HDAC4 is subjected to nuclear cytoplasmic shuttling, also under serum starvation. Incubation with MG132 increased the signal for HDAC4 in both subcellular compartments but did not promote overt changes in its localization.

In nontransformed cells, cell density can induce growth arrest. Hence, we explored whether HDAC4 levels were modulated when growth arrest was induced by density-dependent inhibition. NIH3T3 cells were seeded in 10% FBS, and every 2 d the medium was replaced with fresh 10% FBS. Cytofluorimetric analysis demonstrated that, after 3 d of culture, cells exit the cell cycle and accumulate in G0/G1 phase, similarly to serum-starved cells (Supplemental Figure S1A). Growth arrest was maintained after 7 d of culture (unpublished data). By contrast, HDAC4 protein levels were unchanged during growth arrest induced by density-dependent inhibition (Supplemental Figure S1B).

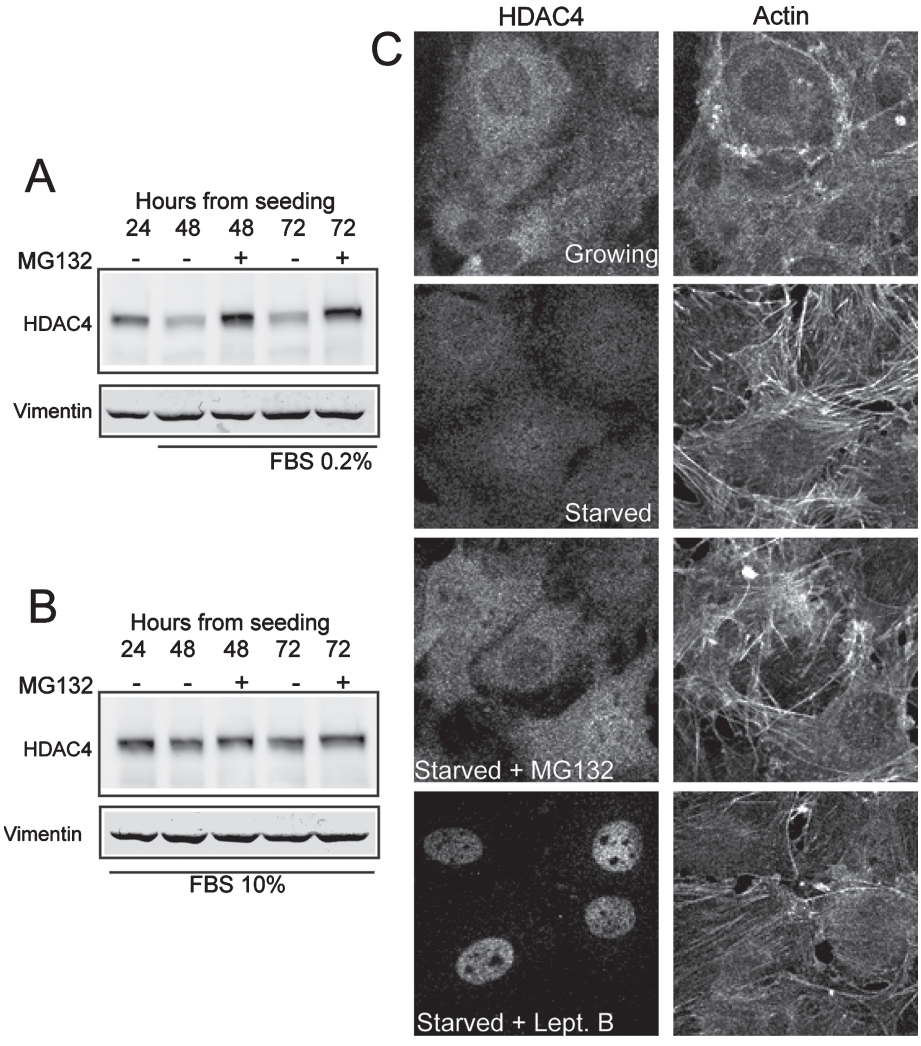

FIGURE 2: Proteasome-dependent degradation of HDAC4 in NIH3T3 cells. (A) NIH3T3 cells were grown for 24 h in 10% FBS (lane 1) and next shifted in low serum (0.2% FBS). When used, MG132 was added to cells 24 h before cell lysis. Cellular lysates were subjected to immunoblot analysis using anti-HDAC4 antibodies. Vimentin was used as loading control. (B) NIH3T3 cells were grown for the indicated times in 10% FBS. When used, MG132 was added 24 h before cell lysis. Cellular lysates were subjected to immunoblot analysis using the specific antibodies. Vimentin was used as loading control. (C) Confocal pictures of growing (24 h after seeding) or serum starved (24 h in 0.2% FBS) NIH3T3 cells. Serum-starved cells were treated with MG132 (2.5 μM) or with leptomycin B (5 ng/ml) for 3 h. Immunofluorescence analysis was performed to visualize HDAC4 subcellular localization. Tetramethylrhodamine-5-(and 6)-isothiocyanate-phalloidin was used to decorate actin filaments.

Conversion of serine 298, sited in PEST1, into an aspartic residue promotes poly-ubiquitination and degradation of HDAC4

PESTs are sequences 10–50 amino acids long containing high densities of Pro, Glu, Ser, and Thr bounded by basic residues that regulate protein stability. Many PEST sequences act as phosphodegrons when they contain phosphorylation sites that mediate interaction with specific E3-ligases. In this manner it is possible to couple substrate degradation to specific environmental signals (Hunter, 2007).

Two PEST sequences (aa 283–331 and aa 559–574) have been described in HDAC4 (Liu *et al.*, 2004). Using the ePESTfind program (http://emboss.bioinformatics.nl/cgi-bin/emboss/epestfind), we confirmed the existence of the two putative PEST sequences. Only in the PEST1 sequence (aa 283–331), however, can consensus phosphorylation sites (serines 298 and 302) be predicted by in silico analysis. Hence, we decided to investigate in more detail the contribution of PEST1 to HDAC4 stability.

We took advantage of HDAC4 derivatives with serines 298 and 302 mutated to

positively charged aspartate residues to mimic constitutive phosphorylation or mutated to alanine residues to mimic constitutive dephosphorylation. To evaluate the destabilizing effect of the Ser/Asp mutations, the different point-mutated versions of HDAC4 fused to green fluorescent protein GFP were transfected in E1A-transformed cells and, following splitting, cells were treated or not with MG132 in the presence of 10% FBS. We also analyzed the behavior of HDAC4 mutated in all three serines recognized by 14–3-3 proteins (HDAC4-TM), which are important to modulate its subcellular localization.

As shown in Figure 3A, levels of the HDAC4 mutant S298D were clearly augmented by treatment with MG132, whereas other mutants and the wild type (WT) were minimally affected. MG132 could promote an increase in the levels of the S302D mutant, albeit less evident compared to the S298D mutant. In this cell line, mutations of the 14–3-3 binding sites do not overtly influence HDAC4 stability.

Hence, we decided to focus our attention on the S298D mutant. To confirm its destabilizing effect and to exclude differences due to transfection efficiency or to the insertion of the GFP tag, we cotransfected HDAC4 and the point-mutated forms S298D and S298A tagged with a FLAG epitope together with GFP, as a standard for transfection efficiency. After transfection, cells were split and treated or not with MG132. As testified by GFP levels, transfection efficiency was similar under the different conditions (Figure 3B). The S298D mutant was expressed at lower levels compared to the WT and the S298A mutant. MG132 treatment evidently increased the amount of the S298D mutant.

To further investigate the prodegradative effect of the mutation S298D we generated NIH3T3 cells stably expressing HDAC4 WT or its point-mutated derivatives S298A and S298D. Figure 3C shows the levels of the different HDAC4-GFP fusions stably expressed in NIH3T3 cells. Surprisingly, inconsistent with the hypothesized prodegradative effect of the S298D mutation, its level was not strongly reduced, compared to those of the WT. Hence we decided to explore whether the similar expression levels of the WT and of the S298D mutant could be ascribed to diverse amounts of the respective mRNAs, as transcribed in the three cell lines. QRT-PCR analysis demonstrated that, in cells expressing the S298D mutant, the relative mRNA was expressed at much higher levels compared to the WT or the S298A mutant (Figure 3D). It is possible that, in the stable cell lines, the intrinsic instability of the S298D mutant is compensated by a higher amount of its mRNA, compared to the mRNAs encoding for the WT or the S298A mutant.

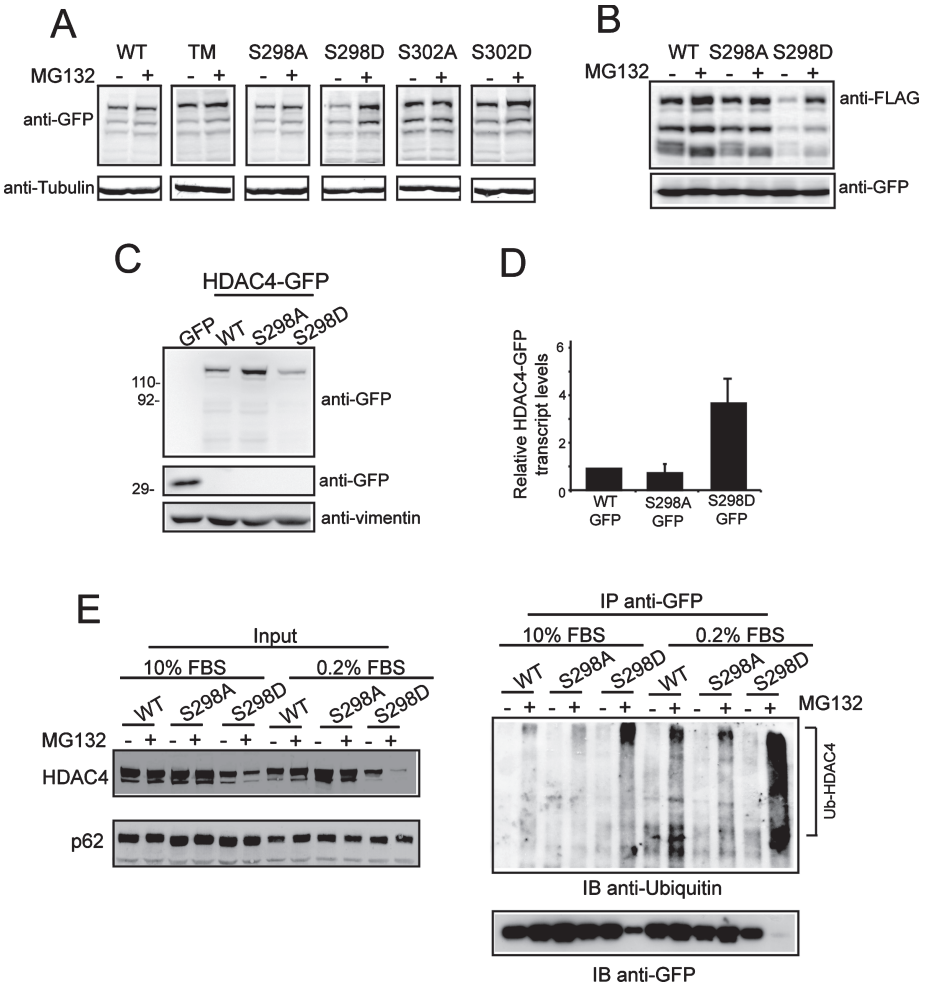

FIGURE 3: Conversion of serine 298 into an aspartic residue, within PEST1 promoted poly-ubiquitination and degradation of HDAC4. (A) Different GFP-fused HDC4 point mutations and the WT form were transfected in IMR90-E1A transformed cells; 24 h later transfected cells were split into two petri dishes and grown for another 24 h. When used MG132 was added 3 h before cell lysis. Cellular lysates were generated and immunoblotted with anti-GFP antibody. Tubulin was used as control. (B) HDAC4 WT and the S298D or A mutants fused to FLAG epitope were cotransfected together with GFP in E1A-transformed cells; 24 h later transfected cells were split into two petri dishes and grown for another 24 h. When used MG132 was added 3 h before cell lysis. Cellular lysates were generated and immunoblotted with anti-FLAG or anti-GFP antibodies. (C) NIH3T3 cells stably expressing GFP or HDCA4 and the S298D/A mutants fused to GFP were lysed, and cellular extracts were subjected to immunoblot analysis using anti-GFP antibodies. Vimentin was used as loading control. (D) Levels of mRNA encoding for HDAC4 or the S298D/A mutants fused to GFP. NIH-3T3 cells were grown in complete medium for 24 h, RNA was extracted, and QRT-PCR analysis was performed to quantify mRNAs of the different fusions. Samples were normalized to β-actin and HPRT (means ± SD, n = 4). (E) NIH3T3 cells stably expressing the different HDAC4-GFP fusions were grown for 24 h in 10% FBS or for an additional 24 h in 0.2% FBS. Cells were lysed as described in *Material and Methods*. HDAC4-GFP fusions were immunoprecipitated using an antibody against GFP and were subjected to immunoblotting using an anti-ubiquitin antibody. After being stripped, the filter was probed with an anti-GFP antibody. When used MG132 was added 3 h before cell lysis. Input has been included, and nucleoporin p62 was used as loading control.

In conclusion, in NIH3T3 cells the S298D mutation achieves a prodegradative influence.

To finally prove the effect of the S298D mutation on protein stability we analyzed the poly-ubiquitination of the different HDAC4-GFP fusions. NIH3T3 cells expressing HDAC4 WT, S298D, or S298A mutants were grown in 10% FBS or in low serum and treated with MG132. After cell lysis, immunoprecipitations were performed using an antibody against GFP. Poly-ubiquitinated

HDAC4-GFP fusions were revealed with an antibody against ubiquitin. Figure 3E proves that the S298D mutant was also poly-ubiquitinated when cells were grown in 10% FBS. Its poly-ubiquitination was dramatically increased in serum-starved cells. The WT protein was poly-ubiquitinated almost exclusively after serum withdrawal, whereas, under the same conditions, the mutant S298A was less poly-ubiquitinated compared to the WT (Figure 3E). Curiously, after MG132 treatment, much less protein was immunoprecipitated in the case of the S298D mutant, possibly because of the high levels of poly-ubiquitination and/or aggresome formation (see later in this article). In conclusion, these studies demonstrate that the mutation S298D within PEST1 promotes poly-ubiquitination and degradation of HDAC4.

Effects of proteasomal inhibition on the subcellular localization of HDAC4 and of the 298 mutants

We have previously demonstrated that the S298D mutation impairs HDAC4 nuclear import (Paroni *et al.*, 2008). To better understand the relationships between nuclear import and proteasomal degradation, we analyzed the subcellular localization of the S298D mutant in cells treated with MG132 by time-lapse analysis. Figure 4A illustrates such analysis. Overall, there was an increase in fluorescence intensity after incubation with MG132. In some cells, the S298D mutant remained in the cytoplasm and, subsequently, aggresome-like structures appeared in the cytosol. In other cells (Figure 4A, arrows), the S298D mutant initially accumulated in the nucleus, but over time aggresome-like structures appeared in the cytoplasm and the nuclear fluorescence decreased. Double immunofluorescence analysis performed in cells expressing HA-ubiquitin demonstrated that aggresomes made by the S298D mutant were positive for ubiquitin (Figure 4B).

To gain further insight into the mechanism responsible for the defective nuclear accumulation of the S298D mutant, we analyzed the subcellular localization of the 298 D/A mutants and of the WT protein, after treatment of the cells with MG132, leptomycin B, or a combination of both drugs. Typical examples of the immunofluorescence analysis are shown in Supplemental Figure S2. In untreated cells, the WT protein was localized into the cytosol. Blocking nuclear export elicited its nuclear accumulation, thus demonstrating that HDAC4 undergoes continuous shuttling. Overall, MG132 treatment did not promote an evident nuclear accumulation of HDAC4, but in some cells the nuclear staining was increased (Supplemental Figure S2). The S298A mutant behaves similarly to the WT (Supplemental Figure S2).

The S298D mutant localizes into the cytoplasm and, as previously demonstrated, blocking nuclear export fails to cause its nuclear accumulation (Supplemental Figure S2). When cells were treated with MG132, the mutant chimera accumulated into aggresome-like structures (Supplemental Figure S2), and a weak nuclear fluorescence could be appreciated in several cells. The addition of leptomycin to cells pretreated with MG132 allowed the nuclear accumulation of the S298D mutant, together with the appearance of cytoplasmic aggregates (Supplemental Figure S2).

To better define the pattern of S298D subcellular localization after MG132 and leptomycin treatment, we decided to perform a time-course analysis. Figure 4C demonstrates that MG132 treatment only weakly affected HDAC4 localization, with ~30% of the cells showing both nuclear and cytoplasmic (pan) localization and rare cells with a prominent nuclear staining. A different pattern was observed for the S298D mutant. In this case, a transient nuclear accumulation was evident (~40% of the cells with nuclear accumulation after a 4-h treatment). The nuclear fluorescence declined with time, and simultaneously cytoplasmic aggresomes became evident (Figure 4C), thus confirming the time-lapse analysis. Importantly, the addition of leptomycin to cells pretreated with MG132 efficiently promoted the nuclear accumulation of the S298D mutant, whereas leptomycin alone was ineffective.

These results indicate that the S298D mutant can be imported into the nucleus, where it becomes susceptible to ubiquitin-dependent proteolysis.

GSK3β is required for starvation-induced proteasomal degradation of HDAC4

Having demonstrated that serine 298 plays a pivotal role in the control of HDAC4 stability and because this serine is a predicted GSK3β target, we used knockout cells for this kinase to evaluate its role in the control of HDAC4 degradation.

GSK3$\beta^{-/-}$ and GSK3 $\beta^{+/+}$ fibroblasts were grown for 48 or 72 h in low serum and treated or not with MG132. Figure 5A evidences that, in GSK3β null cells, HDAC4 levels remained constant, also after 72 h of starvation. In contrast, HDAC4 levels decreased when WT cells were grown in low serum, as previously observed for MCF-10A and NIH3T3 cells. This decrease was suppressed by MG132 treatment.

Next we investigated whether GSK3β could directly phosphorylate HDAC4. For this study we generated a new mutant of HDAC4, in which both serines, 298 and 302, were replaced with alanines. The WT HDAC4 and the different mutants fused to GFP were transfected in 293T cells, and immunoprecipitations were performed with an anti-GFP antibody. GFP was also transfected as a negative control. After immunoprecipitation, the different GFP fusions were incubated in a kinase reaction buffer containing [γ-^{32}P]ATP and recombinant GSK3β. Incubation of WT HDAC4 with GSK3β resulted in significant phosphorylation of the deacetylase (Figure 5B). In the absence of the kinase, HDAC4 was not phosphorylated, thus excluding the contribution of eventually coimmunoprecipitated kinases. Phosphorylation of the double mutant (S298A/S302A) was clearly reduced, thus indicating that these serine residues are indeed GSK3β targets. Interestingly, whereas substitution of serine 298 with alanine did not overtly impaired phosphorylation by GSK3β, mutation of serine 302 dramatically affected HDAC4 phosphorylation. This result suggests that serine 302 could serve as a prime phosphorylation site that promotes subsequent phosphorylation of HDAC4 at serine 298 (Jope and Johnson, 2004).

To verify that comparable amounts of the different HDAC4 mutants were immunoprecipitated, an immunoblot was performed with anti-GFP antibody.

HDAC4 and the cellular responses to serum starvation

The regulation of HDAC4 degradation in response to serum starvation prompted us to investigate whether this enzyme could be implicated in transducing growth factor–related responses. Growth factors affect multiple cellular functions, including proliferation, apoptosis, autophagy, and motility. Hence we decided to unveil which among the listed growth-related activities could be modulated by HDAC4. NIH3T3 cells expressing HDAC4 or GFP were used in comparison. Initially we investigated whether the HDAC4-GFP chimera explicated its repressive influence on myocyte-enhancer factor 2 (MEF2) transcription. We analyzed the mRNA levels of the MEF2 target Krüppel-like factor 2 (KLF2), a member of a subclass of the zinc finger family of DNA-binding transcription factors (Kumar *et al.*, 2005; Wang *et al.*, 2010). The QT-PCR results in Figure 6A show that KLF2 mRNA expression was decreased in NIH3T3 cells expressing HDAC4 compared to GFP. Importantly,

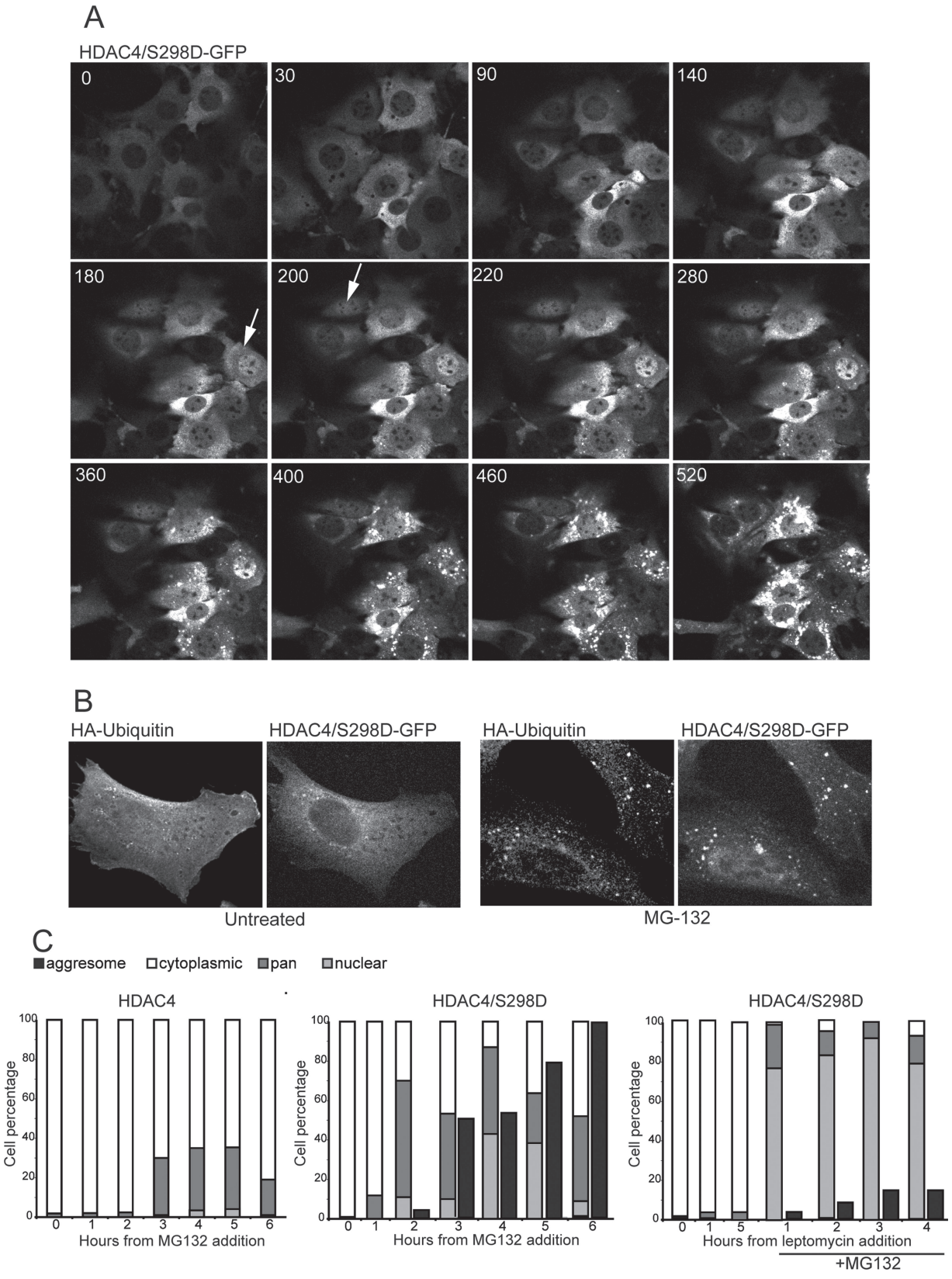

FIGURE 4: Analysis of aggresome formation in NIH3T3 cells expressing the S298D mutant and treated with MG132. (A) Time-lapse analysis of NIH3T3 cell expressing the HDAC4/298D-GFP mutant. Cells were treated with MG132. Frames at selected times (minutes) after addition of MG132 to a representative field are shown. Arrows point to cells that transiently accumulate HDAC4/ S298D-GFP in the nucleus. (B) Confocal microscope images of NIH3T3 cells expressing the HDAC4/S298D-GFP mutant and transfected with HA-tagged ubiquitin. Exponentially growing cells were treated with MG132 for 3 h and then processed for immunofluorescence. (C) Time-course analysis of HDAC4-GFP and HDAC4/S298D-GFP subcellular localization after proteasomal inhibition.

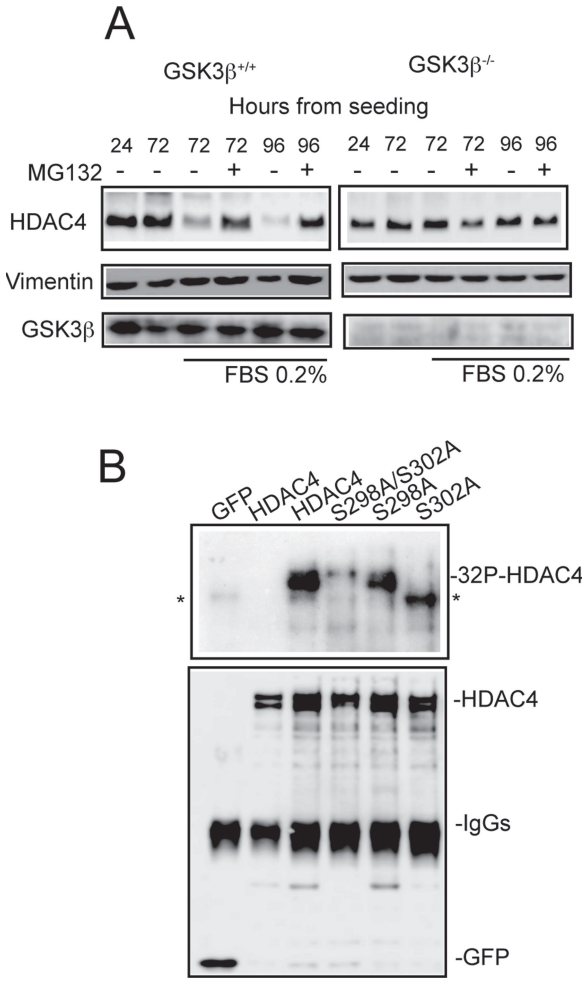

FIGURE 5: GSK3β directly phosphorylates serine 298 and 302 of HDAC4 and modulates its degradation. (A) GSK3β$^{-/-}$ and GSK3 β$^{+/+}$ fibroblasts were grown for 24 h in 10% FBS (lane 1) and next shifted to low serum (0.2% FBS). When used, MG132 was added to cells 24 h before cell lysis. Cellular lysates were subjected to immunoblot analysis using anti-HDAC4 antibodies. Vimentin was used as loading control. (B) Direct phosphorylation of HDAC4 by GSK3β. The top panel shows the result of an in vitro kinase assay after coincubation of recombinant GSK3β with immunoprecipitated HDAC4-GFP, its point mutated versions, or GFP alone, as indicated. In lane 2, WT HDAC4 was incubated in complete kinase assay buffer without the recombinant kinase. The bottom panel shows the loading level of the different immunoprecipitated proteins after immunoblotting with anti-GFP antibody. Asterisks point to a contaminating band.

KLF2 transcript levels were unchanged in cells expressing the S298D mutant, which is defective for repressive activity (Paroni *et al.*, 2008).

Growth factor deprivation can trigger cell death by apoptosis. Hence we evaluated whether cells expressing HDAC4-GFP showed a different susceptibility to apoptosis by low serum conditions. Trypan blue assay and caspase activity (Figure 6, B and C) did not evidence differences in the percentage of apoptosis between serum-starved cells expressing HDAC4-GFP or GFP alone.

In an attempt to adapt to the restrictive environment in terms of nutrients, cells in low serum conditions activate autophagy (Lenk *et al.*, 1999). LC3 (light chain 3) is a specific marker to quantify autophagy in mammalian cells. During autophagy, LC3 undergoes a conversion from the LC3-I isoform to the LC3-II isoform that is specific for autophagosomes (Fontanini *et al.*, 2009). Serum deprivation in NIH3T3 cells induces autophagy (Figure 6D) as evidenced by the appearance of LC3-II. The ectopic expression of HDAC4 did not overtly modulate the appearance of autophagy after serum deprivation.

The main effect of serum starvation in nontransformed cells is the induction of cell-cycle arrest. Hence, we analyzed cell-cycle profiles of cells stably expressing HDAC4-GFP or GFP and grown for different times in low serum. Cytofluorimetric analysis did not reveal changes in the cell-cycle profiles between cells expressing HDAC4-GFP or GFP under the different growth conditions (Figure 6, E–G).

The expression of growth arrest specific (*gas*) genes is up-regulated by serum deprivation. We analyzed the levels of Gas2 protein, which, besides being a marker of G0, is also cleaved by caspase-3 during apoptosis (Brancolini *et al.*, 1995). The immunoblot in Figure 6H confirms that apoptosis was similarly induced in the HDAC4- and GFP-expressing cells, and it also reveals that Gas2 was similarly up-regulated by serum deprivation in the two cell lines.

HDAC4 influences cell motility

Growth factors profoundly affect the architecture of actin cytoskeleton and cell motility. Hence, we finally explored the potential role of HDAC4 in the control of cell motility. Time-lapse microscopy was performed on NIH3T3 cells expressing GFP or HDAC4-GFP, and tracks of individually random migrating cells were analyzed in a computer-aided manner. To evaluate the importance of the MEF2-repressional activity, the motility of cells expressing the S298D mutant was also investigated (Figure 7A). The speed of randomly migrating cells was increased in the presence of HDAC4-GFP compared to GFP alone. Average velocity (arithmetic mean as calculated from the accumulated distance over time) was 0.946 μm/min (SEM = 0.048 n = 78) and 1.468 μm/min (SEM = 0.044; n = 76) for GFP- and HDAC4-GFP–expressing cells, respectively ($p < 0.001$). Interestingly, the random motility of cells expressing the S298D mutant was clearly reduced compared to HDAC4 WT, 1.18 μm/min (SEM = 0.069; n = 54, $p < 0.001$). The difference in migration rate between cells expressing HDAC4 or GFP was even more evident, when data from single-cell analysis were represented as the distance covered by individual cells over time (Figure 7B).

Directional migration is an important component of cell motility that has been shown to be independent from velocity (Pankov *et al.*, 2005). Increased directionality of migration can be quantified by determining the ratio of the shortest, linear distance from the starting point of a time-lapse recording to the end point (D), compared with the total distance traversed by the cell (T) (Pankov *et al.*, 2005). The slight increase in directionality of HDAC4-expressing cells shown in Figure 7C (GFP = 0.33, SEM = 0.025 versus HDAC4 = 0.35, SEM = 0.021) was not statistically significant ($p = 0.38$).

To confirm that HDAC4 regulates random cell motility, we silenced HDAC4-GFP expression. Cells were transfected with small interfering RNA (siRNA) against human HDAC4 or control siRNA. Immunoblot in Figure 7C verified that the siRNA efficiently down-regulated the expression of the HDAC4-GFP transgene. Down-regulation of HDAC4-GFP was coupled to the up-regulation of KLF2 expression, thus confirming that it is an HDAC4 target (Figure 7D).

When we analyzed the speed of randomly migrating cells, overall, a mutual reduction was noted, most likely due to the transfection conditions. Nevertheless, average velocity was significantly reduced in cells transfected with the siRNA against HDAC4 (1.15 μm/min; SEM = 0.056; n = 74) compared to the control (1.35 μm/min; SEM = 0.063; n = 64) ($p < 0.05$).

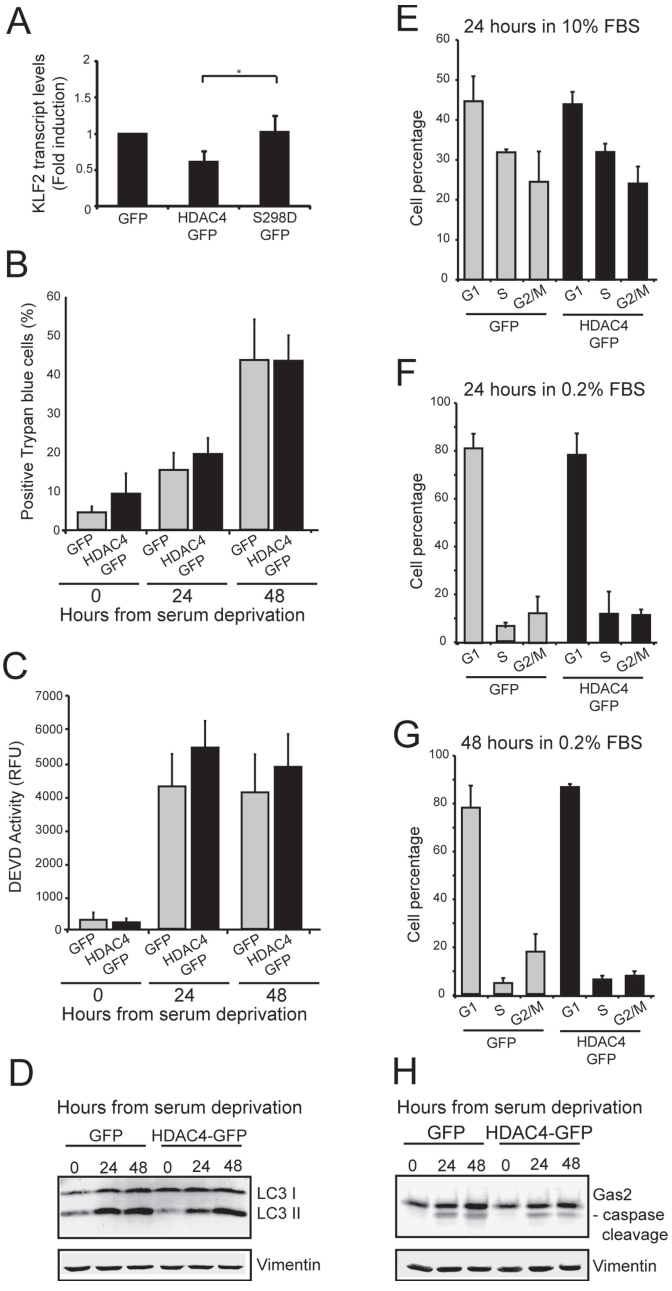

FIGURE 6: Analysis of the cellular responses to low serum conditions in cells expressing HDAC4-GFP. (A) Regulation of KLF2 mRNA expression by HDAC4. RNA was extracted from NIH3T3 cells expressing GFP, HDAC4-GFP, or the point mutant S298D fused to GFP. QRT-PCR analysis was performed to quantify HDAC4 mRNAs. Samples were normalized to GAPDH and HPRT (means ± SD, n = 4). (B) NIH3T3 fibroblasts expressing HDAC4-GFP or GFP were grown for the indicated times in 0.2% FBS. Cell death was scored by trypan blue staining (means ± SD, n = 3). (C) NIH3T3 fibroblasts expressing HDAC4-GFP or GFP were grown for the indicated times in 0.2% FBS. Apoptosis was evaluated by scoring caspase-3/caspase-7 (DEVDase) activities using a fluorogenic assay (means ± SD, n = 3). (D) NIH3T3 fibroblasts expressing HDAC4-GFP or GFP were grown for the indicated times in 0.2% FBS. Equal amounts of cellular lysates were subjected to SDS–PAGE. Immunoblots were performed using an anti-LC3 antibody. Vimentin was used as loading control. (E) Exponentially growing NIH3T3 fibroblasts expressing HDAC4-GFP or GFP were fixed and cell-cycle profiles were assessed after staining with propidium iodide (PI), by fluorescence-activated cell sorting (FACS) analysis (means ± SD, n = 3). (F) After 24 h of serum starvation, NIH3T3 fibroblasts expressing HDAC4-GFP or GFP were fixed, and cell-cycle profiles were assessed after staining with PI, by FACS analysis (means ± SD, n = 3). (G) After 48 h of serum starvation, NIH3T3 fibroblasts expressing HDAC4-GFP or GFP were fixed, and cell-cycle profiles were assessed after PI staining, by FACS analysis (means ± SD, n = 3). (H) NIH3T3 fibroblasts expressing HDAC4-GFP or GFP were grown for the indicated times in 0.2% FBS. Equal amounts of cell lysates were subjected to SDS–PAGE. Immunoblots were performed using an anti-Gas2 antibody. Vimentin was used as loading control.

Finally, we analyzed whether HDAC4 could influence random motility in serum-starved cells. Average velocity was dramatically reduced after 24 h of serum starvation (Supplemental Figure S3) in GFP-expressing cells (0.64 μm/min, SEM = 0.046, n = 54). A similar reduction was observed in the case of WT-expressing cells (0.67 μm/min, SEM = 0.054, n = 43) as well as in S298A-expressing cells (0.69 μm/min, SEM = 0.053, n = 60). These results demonstrate that HDAC4 is not sufficient to counteract the decline in random cell motility, operated by serum withdrawal. Moreover, they indicate that this pathway governing random cell motility is subjected to multiple levels of regulation.

DISCUSSION

HDAC4 degradation

With this work we have added another piece to the complexity of HDAC4 and, more in general, of class IIa HDAC regulation. We demonstrate that serum and growth factors subordinate HDAC4 activity through the control of its ubiquitination and degradation. Serum removal does not influence HDAC4 shuttling, which was similarly observed in growing and starved cells; instead, it elicits HDAC4 poly-ubiquitination and degradation.

Our data reconcile previously published controversial results on proteasome-mediated degradation of HDAC4 (Li *et al.*, 2004; Potthoff *et al.*, 2007). In fact, we have demonstrated that HDAC4 poly-ubiquitination and degradation is a signal-regulated process. It is important to note that HDAC4 degradation could take place not only after serum and/or growth factor removal but also in the presence of serum, when specific signals are provided (Potthoff *et al.*, 2007; Ishikawa *et al.*, 2010).

We have identified specific serines within the PEST1 domain of HDAC4 as important determinants of HDAC4 stability. In particular, mutation of serine 298 into aspartate, which mimics constitutive phosphorylation, causes HDAC4 instability. This mutated HDAC4 is constitutively poly-ubiquitinated and accumulates into aggresomes after proteasomal degradation is suppressed. This behavior is also indicative of an altered protein folding (Rodriguez-Gonzalez *et al.*, 2008). It will be interesting to investigate whether phosphorylation of serine 298 might influence HDAC4 folding and whether this change might represent the switch that allows its poly-ubiquitination.

We previously showed that the S298D mutation affects HDAC4 nuclear import (Paroni *et al.*, 2008). We now demonstrate that when the proteasome is inhibited and leptomycin B is added, this mutant can accumulate into the nucleus. This result indicates that HDAC4 degradation takes place into the nucleus. It would be interesting to investigate whether sumoylation of HDAC4, which occurs during nuclear import, could influence its stability (Kirsh *et al.*, 2002).

The amino acid sequence comprising serines 298 and 302 is highly conserved among class IIa HDACs with the exception of HDAC7. Hence, it is possible that similar mechanisms also operate on HDAC5 and 9 to regulate their stability. In contrast, HDAC7,

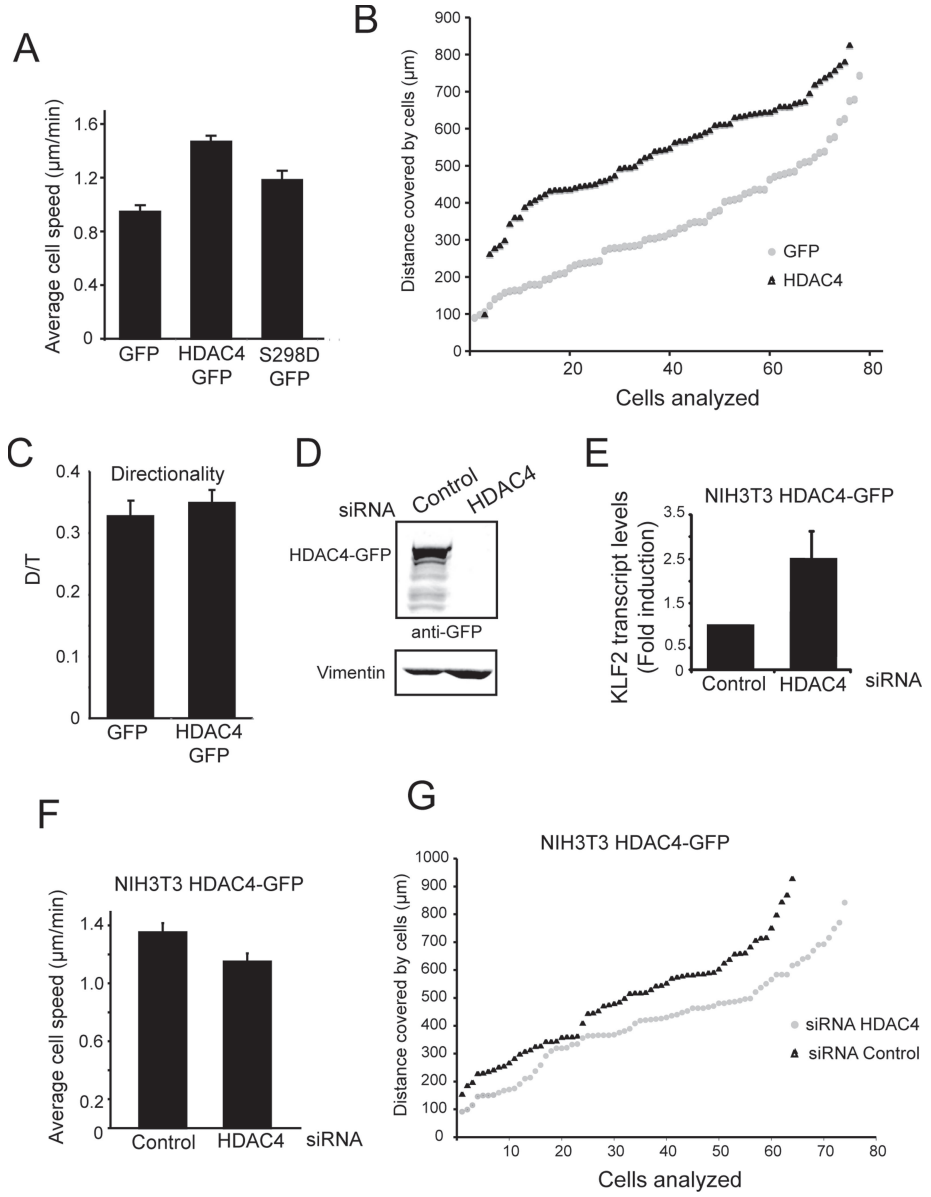

FIGURE 7: HDAC4 influences cell motility. (A) After 24 h from seeding, NIH3T3 cells expressing HDC4-GFP or GFP were subjected to time-lapse analysis for 6 h. Results represent the average migration rate from at least 54 cells from four independent experiments. Cell movements were quantified using MetaMorph software (Molecular Devices, Sunnyvale, CA). (B) Total distance covered by cells expressing GFP or HDAC4-GFP during the time of analysis, as analyzed by time lapse microscopy. Each position along the *x* axis represents a single cell. (C) Quantification of the persistence of migratory directionality. D/T ratios represent the ratio of the direct distance from start to end point (D) divided by the total track distance (T). (D) NIH3T3 cells expressing HDAC4-GFP were transfected with an siRNA against human HDAC4 or a control siRNA. Cellular lysates were generated and immunoblotted with anti-GFP antibody. Vimentin was used as control. (E) NIH3T3 cells expressing HDAC4-GFP were transfected with an siRNA against human HDAC4 or a control siRNA. RNA was extracted, and QRT-PCR analysis was performed to quantify KLF2 mRNA. Samples were normalized to β-actin, and HPRT (means ± SD, n = 4). (F) NIH3T3 cells expressing HDAC4-GFP were transfected with an siRNA against human HDAC4 or a control siRNA; 36 h later, cells expressing HDC4-GFP or GFP were subjected to time-lapse analysis for 6 h. Results represent the average migration rate from at least 64 cells from three independent experiments. (G) Total distances covered by cells expressing HDAC4-GFP and transfected with control or HDAC4 siRNAs are as indicated. After transfection, cells were subjected to time-lapse analysis. Each position along the *x* axis represents a single cell.

which lacks the corresponding serine 298 of HDAC4, could be subjected to different controls (Li *et al.*, 2004). Serines 298 and 302 are placed within consensus sites for GSK3β kinase. GSK3β has been found to regulate the proteolysis of a large number of proteins, in a growth factor–dependent fashion (Xu *et al.*, 2009). We have shown that cells lacking GSK3β are unable to degrade HDAC4 after serum starvation and that GSK3β can phosphorylate HDAC4 in vitro.

GSK3β is unique in requiring a priming phosphate at *n*+4 to phosphorylate many of its substrates (Frame and Cohen, 2001). The double mutation of serines 298/302 into alanines, but also the sole mutation of serine 302, abolishes HDAC4 phosphorylation by GSK3β. These results suggest that serine 302 could act as a priming phosphorylation site. Further studies will be necessary to characterize in detail the pattern of PEST1 phosphorylation and to clearly establish the priming activity of serine 302. Interestingly, in silico analysis highlights that serine 302 could be a substrate both of extracellular-regulated kinase and GSK3β. Hence, control of HDAC4 degradation in cells could undergo a more complex regulation (Zhou *et al.*, 2000).

In summary, proteasomal degradation is a more radical strategy to switch off HDAC4 activity, including "cytosolic functions" (Chen and Cepko, 2009), whereas regulation of nuclear cytosolic shuttling could be more suited for the control of the HDAC4 "nuclear functions."

HDAC4 and cell motility

We have observed that several cellular activities under the control of serum, such as cell-cycle progression, growth arrest, apoptosis, or autophagy, were unaffected by HDAC4. Instead we have noted that random cell motility is augmented in cells expressing HDAC4.

Previous studies have revealed possible roles of class IIa HDACs in the regulation of cell migration and motility. HDAC7 dosage has important implications on endothelial cell motility and migration. Either the silencing of HDAC7 (Mottet *et al.*, 2007) or the overexpression of signal-resistant HDAC7 (mutated in the serine binding sites for 14–3-3) impairs cell motility (Wang *et al.*, 2008). In endothelial cells, siRNA directed against HDAC5 sustained the migration, whereas an opposite effect was exerted by siRNA against HDAC7 and HDAC9. In this model, overexpression of HDAC5 suppressed angiogenesis in an MEF2-independent manner (Urbich *et al.*, 2009). This study confirms a previous report of a negative role of HDAC5 in the control of endothelial cell migration in response to vascular endothelial growth factor (Ha *et al.*, 2008). Although a role of class IIa HDAC in the control of cell motility is emerging, there are some discrepancies. Divergences could be

ascribed to the specific roles of the different HDACs, to the diverse cellular/environmental context, or to the assays used to score cell motility.

Cells can migrate randomly (random cell motility) or can maintain a direction (directionally persistent cell migration) even with no external chemotactic signals, using intrinsic cell migration properties (Pankov *et al.*, 2005; Petrie *et al.*, 2009). In our assay, we have noted that HDAC4 increases cell speed and random cell motility but not directionally persistent migration.

How could HDAC4 modulate cell motility? Genes involved in orchestrating actin cytoskeleton, the expression of which is modulated by HDAC4, are strong candidates to explain the motility effect of the deacetylase. We have shown that, in our cellular model, HDAC4 controls the expression of the MEF2-target gene KLF2. Recent studies have demonstrated that in endothelial cells KLF2 can manage the organization of actin cytoskeleton in response to shear stress (Boon *et al.*, 2010). In cells overexpressing KLF2, focal adhesion kinase was dephosphorylated, and activation of the small GTPase RhoA was amplified (Boon *et al.*, 2010). HDAC4 could antagonize this effect, thus promoting random cell motility.

In addition to the nuclear related functions, we cannot exclude a contribution of the cytosolic HDAC4, which can associate with cardiac myofilaments and modulate the acetylation of Z-disk–associated proteins (Gupta *et al.*, 2008). Moreover, HDAC4 was shown to interact with the actin binding protein α-actinin 4 (Chakraborty *et al.*, 2006; Paroni *et al.*, 2008).

In conclusion, we propose that HDAC4 could modulate the responsiveness to specific mitogenic signals. In our hypothesis, degradation of HDAC4, as triggered by growth factor removal, could be part of the integrated cellular response to fine-tuning its motility to mutated environmental conditions.

MATERIALS AND METHODS

Cell culture

MCF-10A cells were maintained in Ham's F12/DMEM 1:1 medium supplemented with 10% FBS, penicillin (100 U/ml), streptomycin (100 µg/ml), L-glutamine (2 mM), insulin (0.01 mg/ml), hydrocortisone (500 ng/ml), epithelial growth factor (20 ng/ml), and cholera toxin (100 ng/ml). $MEF^{GSK3b-/-}$ $MEF^{GSK\beta+/+}$, IMR90-E1A, MCF-7, 293T, and NIH3T3 cells were maintained in DMEM supplemented with 10% FBS plus penicillin/streptomycin and L-glutamine. The proteasome inhibitor MG132 (Calbiochem, Gibbstown, NJ) was used at 2.5 µM when added for 24 h and at 5 µM when added for 3 or 6 h. The CRM1 inhibitor, leptomycin-B (LC Laboratories, Woburn, MA), was used at 5 ng/ml.

Plasmid construction, transfection, and retroviral infection

pFLAG-CMV5 and pEGFPN1 constructs expressing HDAC4 and its mutants were previously described (Paroni *et al.*, 2008). The double mutant S298A and S302A was generated by in vitro mutagenesis using the Gene-Taylor kit (Invitrogen, Carlsbad, CA) and pEGFPN1-*HDAC4-S298A* as template. Oligonucleotide sequences are available upon request. Plasmid transfections in IMR90-E1A and 293T cells were performed with the calcium phosphate method. NIH3T3 cells expressing the different transgenes were generated by retroviral infection after cloning of *GFP* or GFP-tagged *HDAC4* WT, *HDAC4 S298A*, or *HDAC4 S298D* mutants into pWZL-Hygro retroviral vector, as described previously (Fontanini *et al.* 2009).

Immunoblotting and immunoprecipitation

Proteins obtained after an SDS denaturing lysis and sonication were transferred to a 0.2-µm-pore-sized nitrocellulose membrane and incubated with the following antibodies: anti-HDAC4, anti-GFP, anti-tubulin (Paroni *et al.*, 2004), anti-FLAG-M2 (Sigma Aldrich, St. Louis, MO), anti-vimentin, anti-Gas2 (Brancolini *et al.*, 1995), anti-ubiquitin (Covance, Princeton, NJ), anti-GSK3 (Invitrogen, Carlbad, CA), anti-PCNA (Santa Cruz Biotechnology, Santa Cruz, CA). Blots were then rinsed three times with Blotto/Tween 20 and incubated with the relative secondary antibody (Euroclone, Milan, Italy) for 1 h at room temperature. Blots were then washed three times in Blotto/Tween 20, rinsed in phosphate-buffered saline, and developed with Super Signal West Pico, as recommended by the vendor (Pierce, Rockford, IL).

Immunoprecipitations were performed as previously described (Fontanini *et al.*, 2005). Briefly, cells were collected directly from culture dishes with a rubber scraper into RIPA lysis buffer (50 mM Tris-HCl, pH 8, 150 mM NaCl, 0.2% SDS, 1% Nonidet P-40, 0.5% sodium deoxycholate), supplemented with 50 mM iodoacetamide, 1 µM isopeptidase inhibitor G5 (Fontanini *et al.*, 2009), 1 µM MG132, and protease inhibitors. Lysates were incubated for 6 h with the antibody against HDAC4 or 3 h with the antibody against GFP. After 1 h of incubation with protein A beads (GE, Chalfont St. Giles, UK), washes were performed with RIPA buffer and finally three times with 50 mM Tris-HCl, pH 8. Samples were resolved by SDS–PAGE and analyzed by immunoblot.

In vitro phosphorylation

HDAC4 WT and the different mutants fused to GFP or GFP alone were transfected in 293T cells and immunoprecipitated. After several washes, the different GFP fusions were incubated in the kinase reaction buffer (5 mM 3-(N-morpholino)-propanesulfonic acid [MOPS], pH 7.2, 2.5 mM β-glycerophosphate, 1 mM ethylene glycol tetraacetic acid, 0.4 mM EDTA, 2 mM $MgCl_2$, 50 µM dithiothreitol) containing 10 µM ATP and 300 nM [γ-^{32}P]ATP. Recombinant GST-GSK3β (100 ng; Cell Signaling Technology, Danvers, MA) was added and beads were incubated for 30 min at 30°C. After several washes, samples were resolved by SDS–PAGE, and proteins were transferred to a nitrocellulose membrane. Film exposure to the membrane was used to reveal the amount of phosphorylated proteins, and subsequent immunoblotting of the membrane was used to verify the amount of immunoprecipitated proteins.

RNA extraction and QRT-PCR

Cells were harvested and RNA was obtained using TRIZOL (Invitrogen). RNA integrity was checked by running a formaldehyde-agarose gel. Total RNA (2.5 µg) was used for retrotranscription. QRT-PCR was performed using the Bio-Rad iQ5 or the Bio-Rad CFX96 and SYBR Green technology. To analyze data obtained from QRT-PCR experiments, we used the delta-delta Ct method. In the case of the MCF-10A cells, GAPDH (glyceraldehyde-3-phosphate dehydrogenase) was selected for normalization. In the case of the NIH3T3 cells, the geometric mean of the threshold cycles for HPRT (hypoxanthine phosphoribosyltransferase) and β-actin was selected as the normalization factor. All reactions were done in triplicate. All primer sequences used in this article are available upon request.

Cell-cycle analysis

Cells were detached by trypsin and fixed in 70% ethanol. After some washing, cells were resuspended in PBS supplemented with 1% Triton X-100 and RNAse-A at 100 µg/ml and were incubated for 30 min at 37°C. DNA staining was performed by incubating cells with propidium iodide at 50 µg/ml for 45 min at room temperature. Cells were then passed through a flow cytometer equipped with CellQuest software by using a 488-nm argon ion laser (FACScan; BD Biosciences, Franklin Lakes, NJ). A minimum of 10,000 events per

sample were analyzed. Data analysis was performed by MODFIT software (BD Bioscience, Franklin Lakes, NJ).

Random motility measurements

Random motility was assayed by time-lapse video microscopy analysis of low-density cultured cells. Cells were analyzed at 24 h from plating or at 24 h from starvation. In each experiment, 10× phase contrast time-lapse images were acquired every 15 min during a 6-h period for at least two representative fields for experimental condition. Time-lapse images were analyzed using Metamorph software (Molecular Devices, Sunnyvale, CA). After the center of each cell was defined, its movement was scored throughout the time sequence. The average cell velocity was obtained (μm/min), and the directionality was measured as the ratio between the direct distance from the start to the end point (D) divided by the total track distance (T). Results are pooled from eight independent experiments; error bars indicate SEM based on $N \geq 54$.

ACKNOWLEDGMENTS

We thank Davide Orlando for helping in some experiments and Francesca Demarchi, Laboratorio Nazionale Consorzio Interuniversitario per le Biotecnologie (LNCIB) Trieste, for providing reagents and cell lines. This work was supported by AIRC (Associazione Italiana Ricerca sul Cancro), MIUR (Ministero dell'Istruzione, Università e Ricerca), and Regione Friuli-Venezia Giulia (AITT-LR25/07) to C.B.

REFERENCES

Ago T, Liu T, Zhai P, Chen W, Li H, Molkentin JD, Vatner SF, Sadoshima J (2008). A redox-dependent pathway for regulating class II HDACs and cardiac hypertrophy. Cell 133, 978–993.

Backs J, Song K, Bezprozvannaya S, Chang S, Olson EN (2006). CaM kinase II selectively signals to histone deacetylase 4 during cardiomyocyte hypertrophy. J Clin Invest 116, 1853–1864.

Bolger TA, Yao TP (2005). Intracellular trafficking of histone deacetylase 4 regulates neuronal cell death. J Neurosci 25, 9544–9553.

Boon RA, Leyen TA, Fontijn RD, Fledderus JO, Baggen JM, Volger OL, van Nieuw Amerongen GP, Horrevoets AJ (2010). KLF2-induced actin shear fibers control both alignment to flow and JNK signaling in vascular endothelium. Blood 115, 2533–2542.

Brancolini C, Benedetti M, Schneider C (1995). Microfilament reorganization during apoptosis: the role of Gas2, a possible substrate for ICE-like proteases. EMBO J 14, 5179–5190.

Cadot B, Brunetti M, Coppari S, Fedeli S, de Rinaldis E, Dello Russo C, Gallinari P, De Francesco R, Steinkühler C, Filocamo G (2009). Loss of histone deacetylase 4 causes segregation defects during mitosis of p53-deficient human tumor cells. Cancer Res 69, 6074–6082.

Chakraborty S, Reineke EL, Lam M, Li X, Liu Y, Gao C, Khurana S, Kao HY (2006). Alpha-actinin 4 potentiates myocyte enhancer factor-2 transcription activity by antagonizing histone deacetylase 7. J Biol Chem 281, 35070–35080.

Chen B, Cepko CL (2009). HDAC4 promotes growth of colon cancer cells via repression of p21. Science 323, 256–259.

Choudhary C, Kumar C, Gnad F, Nielsen ML, Rehman M, Walther TC, Olsen JV, Mann M (2009). Lysine acetylation targets protein complexes and co-regulates major cellular functions. Science 325, 834–840.

Cohen TJ, Barrientos T, Hartman ZC, Garvey SM, Cox GA, Yao TP (2009). The deacetylase HDAC4 controls myocyte enhancing factor-2-dependent structural gene expression in response to neural activity. FASEB J 23, 99–106.

Fontanini A, Chies R, Snapp EL, Ferrarini M, Fabrizi GM, Brancolini C (2005). Glycan-independent role of calnexin in the intracellular retention of Charcot-Marie-Tooth 1A Gas3/PMP22 mutants. J Biol Chem 280, 2378–2387.

Fontanini A, Foti C, Potu H, Crivellato E, Maestro R, Bernardi P, Demarchi F, Brancolini C (2009). The isopeptidase inhibitor G5 triggers a caspase-independent necrotic death in cells resistant to apoptosis: a comparative study with the proteasome inhibitor bortezomib. J Biol Chem 284, 8369–8381.

Frame S, Cohen P (2001). GSK3 takes centre stage more than 20 years after its discovery. Biochem J 359, 1–16.

Grozinger CM, Schreiber SL (2000). Regulation of histone deacetylase 4 and 5 transcriptional activity by 14–3-3-dependent cellular localization. Proc Natl Acad Sci USA 97, 7835–7840.

Gupta MP, Samant SA, Smith SH, Shroff SG (2008). HDAC4 and PCAF bind to cardiac sarcomeres and play a role in regulating myofilament contractile activity. J Biol Chem 283, 10135–10146.

Ha CH, Wang W, Jhun BS, Wong C, Hausser A, Pfizenmaier K, McKinsey TA, Olson EN, Jin ZG (2008). Protein kinase D-dependent phosphorylation and nuclear export of histone deacetylase 5 mediates vascular endothelial growth factor-induced gene expression and angiogenesis. J Biol Chem 283, 14590–14599.

Hunter T (2007). The age of crosstalk: phosphorylation, ubiquitination, and beyond. Mol Cell 28, 730–738.

Ishikawa F, Miyoshi H, Nose K, Shibanuma M (2010). Transcriptional induction of MMP-10 by TGF-beta, mediated by activation of MEF2A and downregulation of class IIa HDACs. Oncogene 29, 909–919.

Jope RS, Johnson GV (2004). The glamour and gloom of glycogen synthase kinase-3. Trends Biochem Sci 29, 95–102.

Kirsh O *et al*. (2002). The SUMO E3 ligase RanBP2 promotes modification of the HDAC4 deacetylase. EMBO J 21, 2682–2691.

Kumar A, Lin Z, Senbanerjee S, Jain MK (2005). Tumor necrosis factor alpha-mediated reduction of KLF2 is due to inhibition of MEF2 by NF-κB and histone deacetylases. Mol Cell Biol 25, 5893–5903.

Lenk SE, Susan PP, Hickson I, Jasionowski T, Dunn WA, Jr (1999). Ubiquitinated aldolase B accumulates during starvation-induced lysosomal proteolysis. J Cell Physiol 178, 17–27.

Li X, Song S, Liu Y, Ko SH, Kao HY (2004). Phosphorylation of the histone deacetylase 7 modulates its stability and association with 14-3-3 proteins. J Biol Chem 279, 34201–34208.

Liu F, Dowling M, Yang XJ, Kao GD (2004). Caspase-mediated specific cleavage of human histone deacetylase 4. J Biol Chem 279, 34537–34546.

Liu F, Pore N, Kim M, Voong KR, Dowling M, Maity A, Kao GD (2006). Regulation of histone deacetylase 4 expression by the SP family of transcription factors. Mol Biol Cell 17, 585–597.

Martin M, Potente M, Janssens V, Vertommen D, Twizere JC, Rider MH, Goris J, Dimmeler S, Kettmann R, Dequiedt F (2008). Protein phosphatase 2A controls the activity of histone deacetylase 7 during T cell apoptosis and angiogenesis. Proc Natl Acad Sci USA 105, 4727–4732.

McKinsey TA, Zhang CL, Olson EN (2001). Identification of a signal-responsive nuclear export sequence in class II histone deacetylases. Mol Cell Biol 21, 6312–6321.

Mottet D, Bellahcène A, Pirotte S, Waltregny D, Deroanne C, Lamour V, Lidereau R, Castronovo V (2007). Histone deacetylase 7 silencing alters endothelial cell migration, a key step in angiogenesis. Circ Res 101, 1237–1246.

Pankov R, Endo Y, Even-Ram S, Araki M, Clark K, Cukierman E, Matsumoto K, Yamada KM (2005). A Rac switch regulates random versus directionally persistent cell migration. J Cell Biol 170, 793–802.

Paroni G, Cernotta N, Dello Russo C, Gallinari P, Pallaoro M, Foti C, Talamo F, Orsatti L, Steinkühler C, Brancolini C (2008). PP2A regulates HDAC4 nuclear import. Mol Biol Cell 19, 655–667.

Paroni G, Fontanini A, Cernotta N, Foti C, Gupta MP, Yang XJ, Fasino D, Brancolini C (2007). Dephosphorylation and caspase processing generate distinct nuclear pools of histone deacetylase 4. Mol Cell Biol 27, 6718–6732.

Paroni G, Mizzau M, Henderson C, Del Sal G, Schneider C, Brancolini C (2004). Caspase-dependent regulation of histone deacetylase 4 nuclear-cytoplasmic shuttling promotes apoptosis. Mol Biol Cell 15, 2804–2818.

Petrie RJ, Doyle AD, Yamada KM (2009). Random versus directionally persistent cell migration. Nat Rev Mol Cell Biol 10, 538–549.

Potthoff MJ, Wu H, Arnold MA, Shelton JM, Backs J, McAnally J, Richardson JA, Bassel-Duby R, Olson EN (2007). Histone deacetylase degradation and MEF2 activation promote the formation of slow-twitch myofibers. J Clin Invest 117, 2459–2467.

Rodriguez-Gonzalez A, Lin T, Ikeda AK, Simms-Waldrip T, Fu C, Sakamoto KM (2008). Role of the aggresome pathway in cancer: targeting histone deacetylase 6-dependent protein degradation. Cancer Res 68, 2557–2560.

Sun Y, Ge J, Drnenich J, Zhao Y, Band M, Chen J (2010). Mammalian target of rapamycin regulates miRNA and follistatin in skeletal myogenesis. J Cell Biol 189, 1157–1169.

Tang H, Macpherson P, Marvin M, Meadows E, Klein WH, Yang XJ, Goldman D (2009). A histone deacetylase 4/myogenin positive feedback loop coordinates denervation-dependent gene induction and suppression. Mol Biol Cell 20, 1120–1131.

Urbich C *et al.* (2009). HDAC5 is a repressor of angiogenesis and determines the angiogenic gene expression pattern of endothelial cells. Blood 113, 5669–5679.
Vega RB *et al.* (2004). Histone deacetylase 4 controls chondrocyte hypertrophy during skeletogenesis. Cell 119, 555–566.
Wang AH, Kruhlak MJ, Wu J, Bertos NR, Vezmar M, Posner BI, Bazett-Jones DP, Yang XJ (2000). Regulation of histone deacetylase 4 by binding of 14–3-3 proteins. Mol Cell Biol 20, 6904–6912.
Wang S, Li X, Parra M, Verdin E, Bassel-Duby R, Olson EN (2008). Control of endothelial cell proliferation and migration by VEGF signaling to histone deacetylase 7. Proc Natl Acad Sci USA 105, 7738–7743.
Wang W, Ha CH, Jhun BS, Wong C, Jain MK, Jin ZG (2010). Fluid shear stress stimulates phosphorylation-dependent nuclear export of HDAC5 and mediates expression of KLF2 and eNOS. Blood 115, 2971–2979.
Wilson AJ *et al.* (2008). HDAC4 promotes growth of colon cancer cells via repression of p21. Mol Biol Cell 19, 4062–4075.
Xu C, Kim NG, Gumbiner BM (2009). Regulation of protein stability by GSK3 mediated phosphorylation. Cell Cycle 8, 4032–4039.
Yang XJ, Grégoire S (2005). Class II histone deacetylases: from sequence to function, regulation, and clinical implication. Mol Cell Biol 25, 2873–2884.
Yang XJ, Seto E (2008). The Rpd3/Hda1 family of lysine deacetylases: from bacteria and yeast to mice and men. Nat Rev Mol Cell Biol 9, 206–218.
Zhou X, Richon VM, Wang AH, Yang XJ, Rifkind RA, Marks PA (2000). Histone deacetylase 4 associates with extracellular signal-regulated kinases 1 and 2, and its cellular localization is regulated by oncogenic Ras. Proc Natl Acad Sci USA 97, 14329–14333.